Available online www.jsaer.com

***Journal of Scientific and Engineering Research*, 2019, 6(8):214-237**

Research Article

ISSN: 2394-2630
CODEN(USA): JSERBR

A Critical Analysis of Fast Fourier Transform Technique Used in Automotive Radar Signal Processing Algorithm

***Nathaniel U. Nathaniel[1,2], Evans C. Ashigwuike[2,3], Abubakar U. Sadiq[3,4]**

[1]Department of Computer Engineering, Nile University of Nigeria, Jabi, Abuja, Nigeria
[2]Department of Electrical Electronics Engineering, University of Abuja, P. M. B. 117 Abuja, Nigeria
[3]Department of Electrical Electronics Engineering, Nile University of Nigeria. Jabi, Abuja, Nigeria
[4]National Space Research & Development Agency (NASRDA), Olusegun Obasanjo Space Center Abuja, FCT Nigeria
* Phone: 08060799282, 08182259811, E-mail: nathglobal@yahoo.co.uk, nathaniel@nileuniversity.edu.ng

Abstract This work is about a Critical Analysis of the Fast Fourier Transform (FFT) Technique as used in Automotive Radar Signal Processing (ARSP) Algorithm for Self-Driven Vehicle Applications. One of the applications of radar sensor is in self-driven vehicles. The radar sensor is to detectobstacles and provide accurate information about the vehicle's ambient environment, so as to activate appropriate control commands. This sensor needs a computing platform that can ensure real-time processing of the received signals. Previous works encounter problems in the areas of having appropriate algorithm, chip-set, memory, etc. that are capable of performing these tasks sufficiently. In this work, i. Radar Sensor signal is modeled and simulated. ii. Radar signal for automated driving is simulated using FFT Technique. iii. Analysis on the FFT Technique used is made; in terms of its merits and demerits in this application. All simulations are done using the MATLAB R2017b software. This work will help in creating a more suitable algorithm that process radar sensor signal for self-driven vehicles: it has shown a critical analysis of existing ARSP systems using FFT technique – and the necessity of having a better technique for this application. From this research, I have found out that the major problems with the self-driven vehicle technology using radar sensor are in the areas of appropriate algorithm**,** capable chip-set and sufficient memory; to carry out the task and meet-up with the real-time processing requirement of this application. My work is focused on the area of appropriate algorithm: to analyze the issues and pit-falls in the existing FFT technique used for this application.

Keywords Automotive Radar, Automotive Radar Signal Processing, Fast Fourier Transform, Frequency Modulated Continuous Wave, Modeling, Signal Processing, Simulation

Introduction

Radar systems development started with the experiments carried out by Hertz and Hülsmeyer on the reflections of EMW and ideas advocated by Tesla and Marconiin the late 19th and early 20th centuries, with designs for military and commercial applications: such as air defense purposes—long-range air surveillance, detection of targets, weather studies and forecasting, air traffic control, etc [1-3]. Modern applications of radars in the automotive industry include providing parking assistance, lane departure warning, etc. to the driver. A proposal of self-driven cars considers an extended application of the radar in the automotive industry, whereby cars will have autonomous control of themselves; requiring very little or no assistance from the human passenger using it. For actuators of these controls to function, they must have accurate information of the ambient and on time. This control information will be provided by radar sensors.

Radar sensor is most preferred in this application (than infrared, Bluetooth, sonar, lidar—light detection and ranging, etc.) because of its range of coverage, it is less affected by the weather conditions, its construction and implementation can be made such that the effect of the sensor to the vehicle's aerodynamics and appearance is not detrimental [4-6]. Radar sensors use Frequency Modulated Continuous Wave (FMCW) to reliably detect moving or stationary targets. Radar based sensors are ideal for collision avoidance on board mobile equipment. An example is the R-Gage Series Radar Sensor which is a high sensitivity radar-based sensor, ideal for collision avoidance on board mobile equipment [4].

In processing the radar sensor signals, some of the issues with the FFT technique as captured from reviewed literatures, stated below, are the case to be used for this critical analysis. In [4], **i.** Fast Fourier Transform is the core process of the algorithm; **ii.** The algorithm requires huge amount of intermediate data to be stored in a memory; **iii.** Memory transpose operation might be required in order to have an efficient memory access; **iv.** The on-chip memory provided by Virtex-6 FPGA (a module used) was found to be insufficient for the storage of the intermediate data. Thus, it has been decided to use the off-chip SDRAM memory for this purpose. This constraint would require transpose operation to be performed in the memory. As it was discovered later, this operation would be the main bottleneck of the implementation. These are the basis of the necessity for the proposal of the use of the WT technique for this application: it is shown that WT technique will overcome most of the FFT technique demerits.

The software for this work, MATLAB is preferred because of its vast capabilities and flexibilities for designs and simulations required. However, in this work, MATLAB R2017b is used and these products are involved mostly in the designs and simulations: *MATLAB and Simulink, Automated Driving System Toolbox, Phased Array System Toolbox*, etc. This is because the concept of self-driven vehicles is a 'work-in-progress'; most of the tools needed to accurately implement the technology are not yet in place, which is why this work is carried out to contribute in the area of processing the radar sensor signal – where the radar sensor is one of the most crucial components.

Involved in the conversion of the output of the signal processing (by FFT or WT), [1] are the three basic DSP steps namely: Representing the signals by a sequence of numbers-Sampling or analog-to-digital conversions; Performing processing on these numbers with a digital signal processor-Digital signal processing; Reconstructing analog signal from processed numbers-Reconstruction or digital-to-analog conversion, as shown in the block diagram, fig. 1 below.

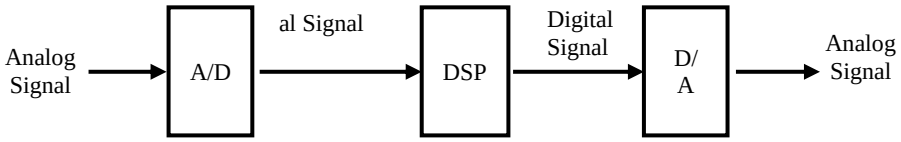

Figure 1: The three basic DSP steps

Definition of Key Terms

RADAR (RAdio Detection And Ranging) – Basically radar can be defined as a system for detecting the presence, direction, distance, and speed of aircraft, ships, and other objects, by sending out pulses of radio waves which are reflected off the object back to the source.

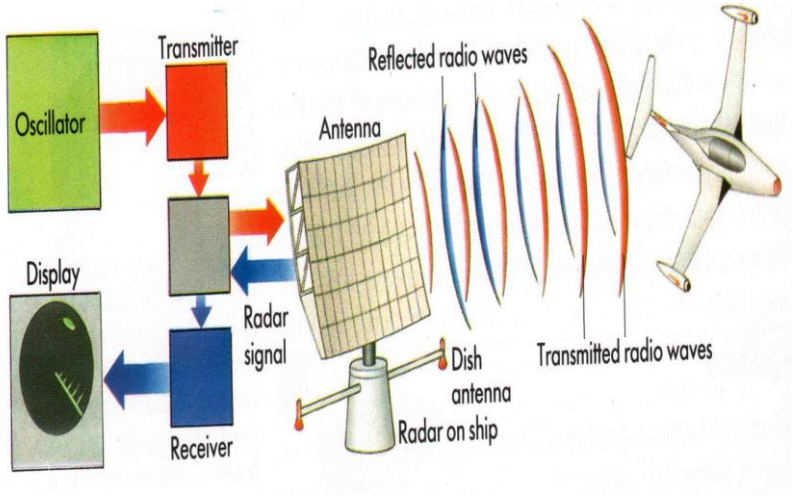

Figure 2: RADAR Working Principle

Radar Types include – Bistatic: the transmit and receive antennas are at different locations as viewed from the target (e.g., ground transmitter and airborne receiver). Monostatic: the transmitter and receiver are colocated as viewed from the target (i.e., the same antenna is used to transmit and receive).Quasi-monostatic: the transmit and receive antennas are slightly separated but still appear to be at the same location as viewed from the target (e.g., separate transmit and receive antennas on the same aircraft) [8].

NORMAL RADAR FUNCTIONS include: Range (from pulse delay), Velocity (from Doppler frequency shift), Angular direction (from antenna pointing), Signature analysis and inverse scattering, Target size (from magnitude of return), Target shape and components (return as a function of direction), Moving parts (modulation of the return), Material composition. The complexity (cost & size) of the radar increases with the extent of the functions that the radar performs [8].

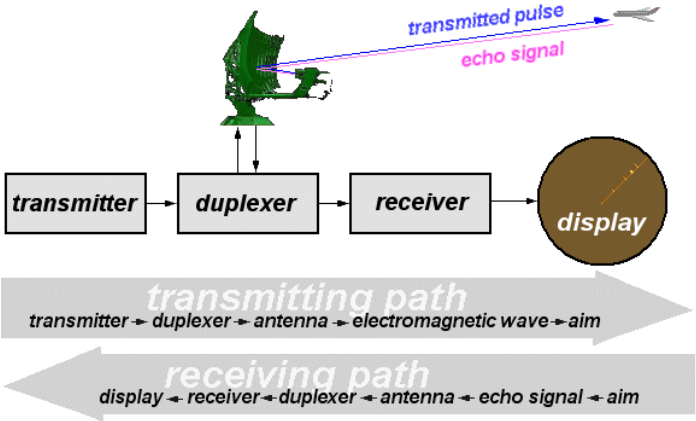

Figure 3: Block diagram of a primary radar with the signal flow

RADAR MEASUREMENTS include: Metric Coordinates of Detected Targets [Range: R = $c\tau$/ 2; where c = speed of light, m/s, τ= round-trip echo time, s], [Range Rate: $v_r = \lambda f_d/2$ where, v_r = target radial velocity, m/s, λ=wavelength of RF Transmit pulse, m, f_d= Doppler frequency shift of echo, Hz], [Azimuth / Elevation θ, Φ], [Position of antenna beam at time of detection]. Special-Purpose Radar Measurements –Target Motion Spectra; Modulation of Doppler shift by target motion;

– Synthetic Aperture Radar; Conversion of Doppler shift to angle offset

RADAR SIGNAL PROCESSING Extensive usage of DSP concepts

1. How to find range of the object/Target is by Time Domain Processing (Band Pass Sampling)

2. How to find the speed of the object/Target is by Frequency Domain Processing (DFT/FFT)
3. How to achieve desired range resolution is by Frequency Domain Processing (Fast Convolution, Windowing).
4. How to suppress unwanted signal/Clutter is by Frequency Domain Processing (Finite Impulse Response [FIR] Filters) [9], also see [10].

SIGNAL PROCESSING: *Signal processing* basically concerns with the analysis, synthesis, and modification of *signals*, which are broadly defined as functions conveying "information about the behavior or attributes of some phenomenon", such as sound, images, etc. [11].

AUTOMOTIVE RADAR: Radar used for automotive applications especially in self-driven vehicles. Automotive radars, along with other sensors such as lidar, ultrasound, and cameras, form the backbone of self-driving cars and ADAS: They are responsible for the detection of objects and obstacles, their position, and speed relative to the vehicle. Various signal processing techniques have been developed to provide better resolution and estimation performance in all measurement dimensions: range, azimuth-elevation angles, and velocity of the targets surrounding the vehicles. There are various aspects of automotive radar signal processing techniques, including waveform design, possible radar architectures, estimation algorithms, implementation complexity-resolution trade off, and adaptive processing for complex environments, as well as unique problems associated with automotive radars such as pedestrian detection [2], [3].

FUNDAMENTALS OF RADAR SIGNAL PROCESSING: What does the Radar sensor do?

The efficiency of the self-driven vehicle system is based on its performance in terms of target detection and identification; which in turn is dependent on the information extracted from the sensor signal (a time domain signal): so it is crucial to adopt a more suitable transformation technique which is best to extract the relevant information from the signal. The received signal has some important information relating to the ambient, hidden in it and cannot be used directly by actuators in this application. Transformation techniques like the Wavelet transform, Fourier transform, Laplace transform and Z transform; are used to reveal this information. The transformation through Fourier and Laplace transform, information about the frequency can be achieved while by applying wavelet transform, information about frequency, time and scale can be attained. Once the signal has been transformed, the similarity and dissimilarity of the target's signature can easily be observed. To get better information, the right transformation technique should be used [5]. The signals are processed for the purposes shown in fig. 4 below.

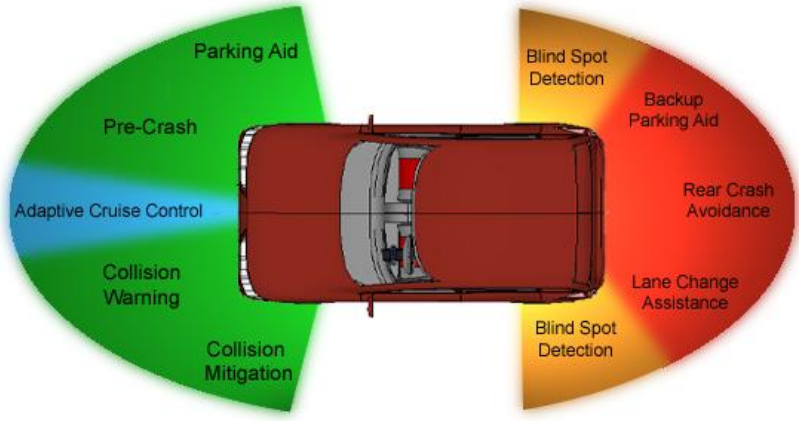

Figure 4: What radar sensor process signals for

The Fourier Transform (FT): The FT pairs as we know, is given by:

$$x(t)=\int_{-\infty}^{\infty} X(\omega)e^{j\omega t}d\omega \quad \longleftrightarrow \quad X(\omega)=\frac{1}{2\pi}\int_{-\infty}^{\infty} x(t)e^{-j\omega t}dt$$

Dirichlet condition which state that: 1. On any finite interval, *f(t)* is bounded; *f(t)* has a finite number of maxima and minima; *f(t)* has a finite number of discontinuities. 2. *f(t)* is absolutely integrable. These are sufficient and not necessary conditions: some functions like cos(ωt) may not be absolutely integrable but has FT. The FT is used to simplify the calculation of the response of linear systems to input signals; it also allows the use of

algebraic equations to analyze systems that are described by linear time-invariant differential equations. It has properties such as Linearity, Time-Scaling, Time Shifting, etc.

FAST FOURIER TRANSFORM (FFT): Let's consider FT in terms of space and time:

Space	
x	space variable
L	spatial wavelength
$k=2\pi/\lambda$	spatial wavenumber
F(k)	wavenumber spectrum

Time	
t	Time variable
T	period
f	frequency
$\omega=2\pi f$	angular frequency

With the complex representation of sinusoidal functions e^{ikx} (or (e^{iwt}) the Fourier transformation can be written as:

$$F_k = \frac{1}{N}\sum_{j=0}^{N-1} f_j e^{-2\pi ikj/N}, k = 0,1,..., N-1$$

$$f_k = \sum_{j=0}^{N-1} F_j e^{2\pi ikj/N}, k = 0,1,..., N-1$$

$$f(x) = \frac{1}{\sqrt{2\pi}}\int_{-\infty}^{\infty} F(k)e^{-ikx}dx$$

$$F(k) = \frac{1}{\sqrt{2\pi}}\int_{-\infty}^{\infty} f(x)e^{ikx}dx$$

Whatever we do on the computer with data will be based on the discrete Fourier transform

The FT approach became interesting with the introduction of the FFT. But what's so fast about it? The FFT originates from a paper by Cooley and Tukey (1965, Math. Comp. vol 19 297-301) which revolutionized all fields where FT where essential to progress.

The FFT can be written as matrix-vector products. For example, the inverse transform yields;

$$\begin{bmatrix} 1 & 1 & 1 & 1 & \dots & 1 \\ 1 & \omega & \omega^2 & \omega^3 & \dots & \omega^{N-1} \\ 1 & \omega^2 & \omega^4 & \omega^6 & \dots & \omega^{2N-2} \\ \vdots & \vdots & & & & \vdots \\ \vdots & \vdots & & & & \vdots \\ 1 & \omega^{N-1} & \dots & \dots & \dots & \omega^{(N-1)^2} \end{bmatrix} \begin{bmatrix} \hat{u}_0 \\ \hat{u}_1 \\ \hat{u}_2 \\ \vdots \\ \vdots \\ \hat{u}_{N-1} \end{bmatrix} = \begin{bmatrix} u_0 \\ u_1 \\ u_2 \\ \vdots \\ \vdots \\ u_{N-1} \end{bmatrix}$$

Where $\omega = e^{2\pi i/N}$

The FAST bit is recognizing that the full matrix - vector multiplication can be written as a few sparse matrix - vector multiplications (for details see for example Bracewell, the Fourier Transform and its applications, MacGraw-Hill) with the effect that:

Number of multiplications	
Full Matrix	FFT
N^2	$2N\log_2 N$

This has enormous implications for large scale problems. Note: the factorization becomes particularly simple and effective when N is a highly composite number (power of 2).

Table 1: FFT

Number of multiplications			
Problem	**Full Matrix**	**FFT Ratio**	**Full Matrix/FFT**
1D (nx=512)	$2.6x10^5$	$9.2x10^3$	28.4
1D (nx=2096)			94.98
1D (nx=8384)			312.6

The right column can be regarded as the speedup of an algorithm when the FFT is used instead of the full system [10, 12–14].

HOW RADAR DETERMINES RANGE AND VELOCITY OF TARGETS: Basically, how does Radar determine range and velocity of targets accurately, even in the presence of noise? If we create a signal to transmit and simulate return signals, adding noise and Doppler shift and detect returned burst with Matched filter. Time delay in the returned signal can be Utilize to determine range: performing spectral analysis and using Doppler Effect, velocity can be calculated. The radar transmitter sends out a burst signal which hits the target. The speed of the target shifts the signal according to the Doppler equation. The radar then receives the reflected signal.

For Range: the system measures time for the return signal to arrive, thus; Range = (1/2c) *T_d, where T_d = time delay. For Velocity: the system measures Doppler shift, thus;

Velocity = $(f_dc)/(2f_c)$, where f_c = frequency of radar f_d = Doppler frequency shift.

The block diagram for Radar Processing is shown below:

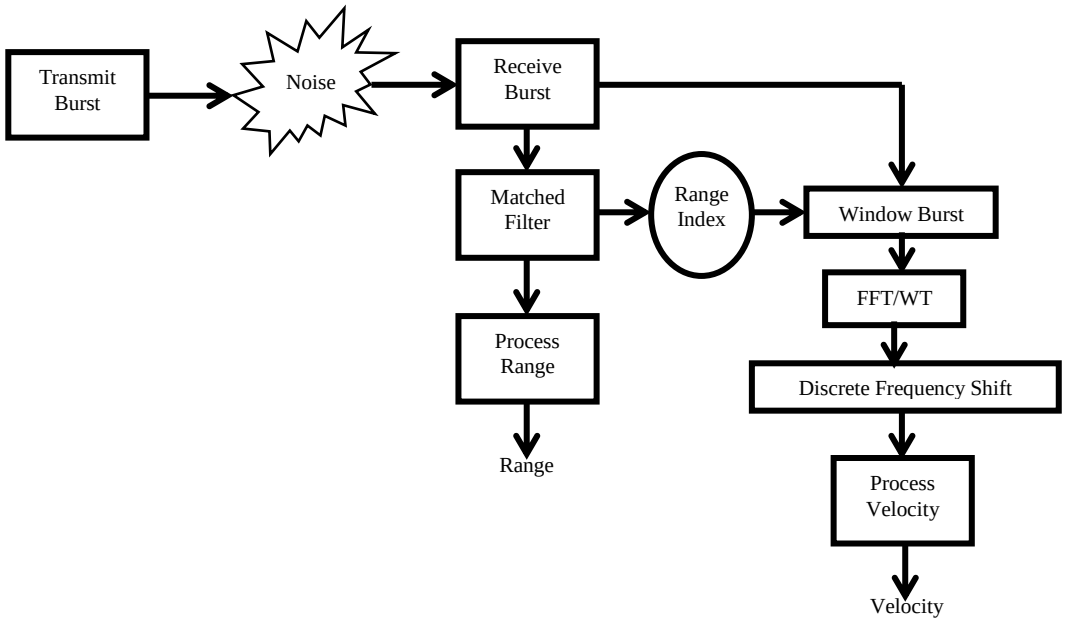

Figure 5: Block Diagram for Radar Processing

Review of Relevant Similar Works

I. FMCW Radar signal processing module for automotive applications –in [4], "Design and implementation of an FMCW Radar signal processing module for automotive applications". In his work, the subject of his thesis was to investigate the processing platforms for the real-time signal processing of the automotive FMCW radar developed at the NXP Semiconductors. The radar sensor is designed to be used in the self-driving vehicles. The thesis first investigates the signal processing algorithm for the MIMO FMCW radar. It is found that the signal processing consists of the 3D FFT processing. It was found that the multiprocessor system is not capable to meet the real-time constraints of the application [4].

The results of the implementation show that the architecture can provide reliable outputs regarding the range, velocity and bearing information. The accuracy of the results is limited by the range, velocity and angular

resolution which are determined by the specific parameters of the RF front-end and the designed waveform pattern. However, the real-time performance on the architecture cannot be achieved due to the high latencies introduced by the memory transpose operations. A few techniques have been tested to decrease the latency bottleneck caused by the SDRAM transpose processes; however, none of them have shown any significant improvements [4].

Most books and articles on WT are written by math people, for the other math people; still most of the math people don't know what the other math people are talking about (a math professor's confession). Why do we need a transform? Mathematical transformations are applied to signals to obtain further information from that signal that is not readily available in the raw signal. Most of the signals in practice are time-domain signals in their raw format. When we plot time-domain signals, we obtain a time-amplitude representation of the signal. This representation is not always the best representation of the signal for most signal processing related applications. In many cases, the most distinguished information is hidden in the frequency content of the signal. The frequency SPECTRUM of a signal is basically the frequency components (spectral components) of that signal. The frequency spectrum of a signal shows what frequencies exist in the signal [4, 14].

FT is normally used to find the frequency content of a signal. If the FT of a signal in time domain is taken, the frequency-amplitude representation of that signal is obtained. For most practical purposes, signals contain more than one frequency component. The frequency spectrum of a real valued signal is always symmetric. Why do we need the frequency information? Often times, the information that cannot be readily seen in the time-domain can be seen in the frequency domain.

Although FT is probably the most popular transform being used (especially in electrical engineering), it is not the only one. There are many other transforms that are used quite often by engineers and mathematicians. Hilbert transforms, short-time Fourier transform, Wigner distributions, the Radon Transform, the wavelet transform, etc. Every transformation technique has its own area of application, with advantages and disadvantages. FT is a reversible transform, that is, it allows going back and forwarding between the raw and processed (transformed) signals. However, only either of them is available at any given time. That is, no frequency information is available in the time-domain signal, and no time information is available in the Fourier transformed signal. The natural question that comes to mind is that is it necessary to have both the time and the frequency information at the same time? The answer depends on the particular application and the nature of the signal in hand. FT gives the frequency information of the signal, which means that it tells us how much of each frequency exists in the signal, but it does not tell us when in time these frequency components exist. This information is not required when the signal is stationary. Stationarity is of paramount importance in signal analysis. Signals whose frequency content does not change in time are called stationary signals. In other words, the frequency content of stationary signals does not change in time. In this case, one does not need to know at what times frequency components exist, since all frequency components exist at all times [14–22].

Now, consider non-stationary signal, the frequency components change continuously. Therefore, for these signals the frequency components do not appear at all times! Other than the ripples, and the difference in amplitude (which can always be normalized), the two spectrums are almost identical, although the corresponding time-domain signals are not even close to each other. Both of the signals involve the same frequency components, but the first one has these frequencies at all times, the second one has these frequencies at different intervals. So, how come the spectrums of two entirely different signals look very much alike? Recall that the FT gives the spectral content of the signal, but it gives no information regarding where in time those spectral components appear. FT is not a suitable technique for non-stationary signal, with one exception: FT can be used for non-stationary signals, if we are only interested in what spectral components exist in the signal, but not interested where these occur. However, if this information is needed, i.e., if we want to know, what spectral component occur at what time (interval), then Fourier transform is not the right transform to use. FT gives what frequency components (spectral components) exist in the signal. No more, no less. When the time localization of the spectral components is needed, a transform giving the time-frequency representation of the signal is needed. The ultimate solution: the wavelet transform [14-23].

II. FMCW systems in MATLAB – FMCW system consists of a transmitter, receiver and mixer basically. When a modulated signal is transmitted and received, they are multiplied in the time domain and processed. From the

work in [24], the system model is flows thus: 1) Calculate transmitted signal; 2) Calculate received signal; 3) Mix signals (multiply in time domain); 4) Two sinusoidal terms are derived; filter out one; 5) Perform FFT on filtered signal; 6) Improved spectrum output with windowing, zero padding; 7) Possibly perform additional post-processing. The flow can be shown in the block diagram of Fig. 6 below;

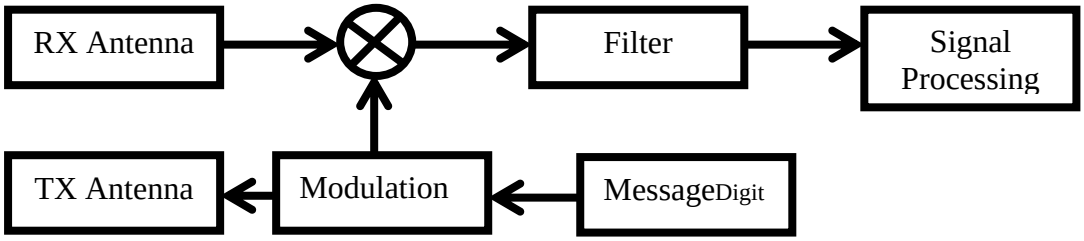

Figure 6: Basic FMCW system

The FMCW used in MATLAB is possible with three modulation schemes: Sawtooth, Triangular and Sinusoidal. We know that frequency modulation is defined by; $S_t = \cos(2\pi f_c t + \int_0^t f_{sig} d\tau)$

Where f_c is the carrier frequency and is the signal that the carrier frequency is modulated with f_{sig} the maximum or minimum difference between the modulated signal and the carrier frequency is $\pm\Delta f$. This equation demonstrates the transmitted frequency; the received frequency is delayed by

$$t_d = \frac{2\Delta f R(t)}{cT} \; ; \qquad \text{With } R(t) = \frac{Ro}{T/2} + vt$$

And is also doppler-shifted by $f_d = 2vf_c/c$, where T is the period of the modulation signal. Since the frequency modulated signal is periodic, the following analyses are performed for one period of the modulation. Each of the following scenarios has this same basic modulation algorithm, but in the end, all have different methods for deriving the range and velocity. Different scenarios work best for each modulation scheme, and so all three systems make use of different point scatters and have different system characteristics [24-26].

III. FMCW Radar Signal Analysis – Why use the FMCW waveform; why not rectangular pulse or any other waveform? Radars that use rectangular pulse waveform are larger and are suitable for military applications; they have long distance target detection coverage. Automotive radar systems often adopt FMCW technology because FMCW radars are smaller, use less power, and are much cheaper to manufacture compared to pulsed radars. As a consequence, FMCW radars can only monitor a much smaller distance which is just appropriate for our design here, 200m coverage is well enough for automotive application [24-26].

Figure 7a: FMCW LoS Propagation Model

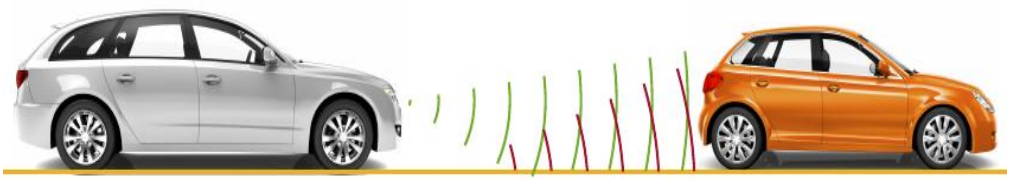

Figure 7b: FMCW Multi-Path Propagation Model

In this work, Modeling, Simulation and Analysis of ARSP using FFT technique is carried out. The technique is analyzed critically, to show its merits and demerits in this application. It is aimed at creating a more suitable algorithm that process radar sensor signal for self-driven vehicles, with main objectives to: illustrate how ARS is processed using FFT technique; analyzed critically FFT technique as used for this application; show the demerits of using FFT technique ARSP. I am motivated to carry out research in this area because of my passion for automation systems: making them work with less human intellectual involvement in their basic operations and without costly errors. For instance, my concern was drawn to an incident in early 2018, where Uber self-

driven vehicle on a test mission, knocked down and killed a pedestrian in Florida, USA. One of the areas to look into, for the possible causes of that incident is the signal processing technique and algorithm. Dashcam video showed the backup driver looking down at her lap seconds before the crash [27]. The organization of this work is thus: the summary is presented in the abstract section, then the general introduction, methodology, results and analysis, then the conclusions. Some proposed solutions of the FFT technique demerits from this analysis are presented in my earlier work in [28].

Methodology—Modeling and Simulations [details are captured in my thesis work].

I. Basic Concepts for End-to-End Radar System Design: The following models are carried out: Waveform Model, Antenna Model, Target Model, Antenna & Target Platforms, Modeling Transmitter, Modeling Waveform Radiation & Collection, Modeling Receiver, Modeling Propagation and Implementing the Basic Radar Model. This model shows how radar detect the range of a target.

II. Radar Sensor Detections: What parameters of the target radar sensor should detect and giving it an appropriate algorithm to do so; based on some MATLAB R2017b documentation. The following radar sensor detections are considered: Target detection; FCW Driving Scenario; Forward-Facing Long-Range Radar; Radar Detections (i.e. Moving and Stationary Targets); Target Range estimation (i.e. Position Measurement); Target Velocity Estimation (i.e. Velocity Measurement); Radar Velocity Measurements Configuration; Target Angle Estimation (i.e. Azimuth); Targets Identification (i.e. Pedestrian & Vehicle Detection);FCW Driving Scenario with a Pedestrian and a Vehicle; Configuration of Radar Detections Performance; Mid-Range Radar Detections Performance; Detection of Closely Spaced Target. To analyze the differences between radar measurements and the vehicle ground truth position and velocity for FCW scenario, a passing vehicle scenario, and a scenario with closely spaced targets are modeled: it also includes a comparison of SNR values between pedestrian and vehicle targets at various ranges; [29, 30-38].

III. Automotive Adaptive Cruise Control Using FMCW Technology: models considered are; FMCW Waveform; Target Model; Radar System Setup; Range and Doppler Estimation; Range Doppler Coupling Effect; Triangular Sweep; Two-ray Propagation. The received signal is a time-delayed copy of the transmitted signal where the delay, Δt, is related to the range.

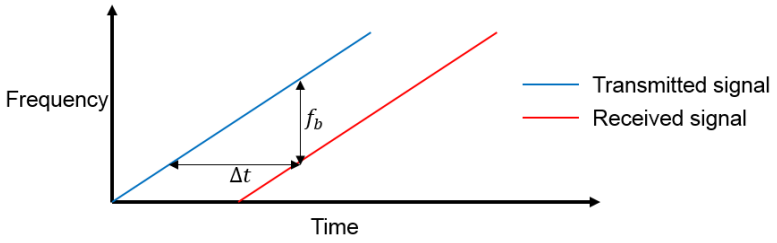

Figure 8: FMCW Range Measurement Principle

A summary of the parameters configuring the FMCW radar used in this modeling is given below:

Table 2: Parameters configuring the FMCW radar

System Parameters	Value	Unit
Operating frequency	77	GHz
Maximum target range	200	m
Range resolution	1	m
Maximum target speed	230	Km/h
Sweep time	7.33	µsec
Sweep bandwidth	150	MHz
Maximum beat frequency	27.30	MHz
Sample rate	150	MHz

Triangular sweep has one up sweep and one down sweep to form one period, See Fig. 9 below; by combining the beat frequencies from both up and down sweep, the coupling effect from the Doppler can be averaged out and the range estimate can be obtained without ambiguity.

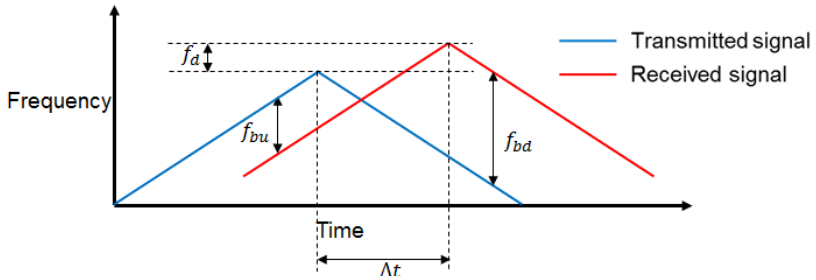

Figure 9: Triangular sweep

The two-ray model describes a multipath scenario the signal propagates from the radar to the target vehicle via two paths, one direct path and one reflected path off the road, see fig. 7 above, [1, 39-46].

IV. Automotive Radar Sensor Signal Processing (with FFT): models considered are; Calculation of Radar Parameters from Long-Range Radar Requirements; Automotive Radar Hardware; Radar Signal Processing Chain; Free Space Propagation Channel; Driving Scenario; Multipath Channel [34, 40-41, 44-45, 47-55].

Results and Analysis

I. Result of Basic Concepts for End-to-End Radar System Design: the red vertical line on the plot of fig. 10 below marks the range of the target.

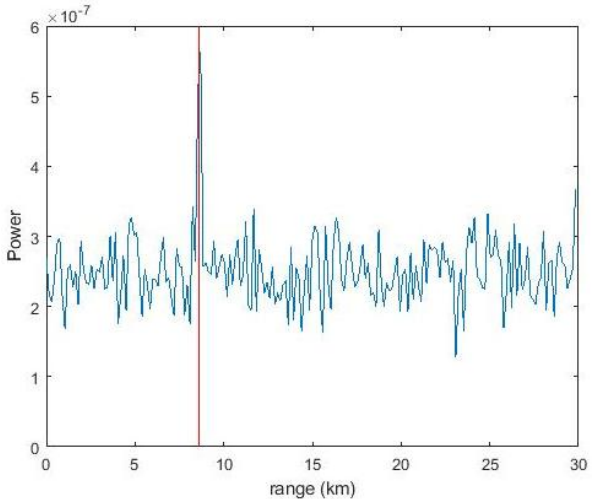

Figure 10: Implementing the Basic Radar Model

II. Results of Radar Sensor Detections: (i) Radar detection-as designed, deceleration start according to the sensor range resolution, the ego vehicle come to a complete stop 2m before the target vehicle's rear bumper.

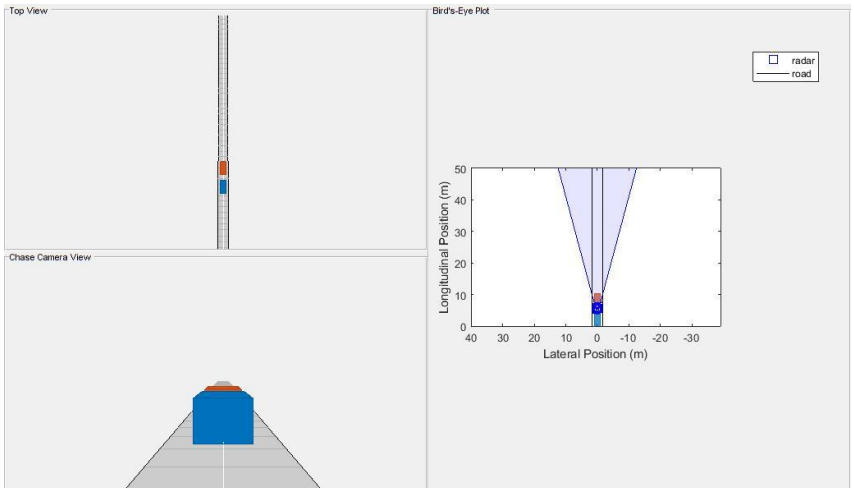

Figure 11: ego vehicle stops 2m before the target vehicle's rear bumper

(ii) Target Range estimation-for a forward-facing radar configuration, the radar's range measurements correspond to the longitudinal position of the target vehicle. The longitudinal position errors in the resulting plot of fig. 12 (left), shows about -1 meter bias between the longitude measured by the radar and the target's ground truth position. This bias indicates that the radar consistently measures the target to be closer than the position reported by the ground truth. Instead of approximating the target as a single point in space, the radar models the physical dimensions of the vehicle's body. Detections are generated along the vehicle's rear side according to the radar's resolution in azimuth, range, and (when enabled) elevation. This -1 meter offset is then explained by the target vehicle's rear overhang, which defines the distance between the vehicle's rear side and its rear axle, where the ground truth reference is located: the stationary vehicle rear did not overhang since we used 2m stop for the ego vehicle. The radar is modeled with a range resolution of 3 meters. However, the 2σ measurement noise is reported to be as small as 0.3 meter at the closest point and grows slightly to 0.7 meter at the farthest tested range. The realized sensor accuracy is much smaller than the radar's range resolution. Because the radar models the SNR dependence of the range errors using the Cramer-Rao lower bound, targets with a large RCS or targets that are close to the sensor will have better range accuracy than smaller or more distant targets. This SNR dependence on the radar's measurement noise is modeled for each of the radar's measured dimensions: azimuth, elevation, range, and range rate.

The lateral position errors fig. 12 (right) shows a strong dependence on the target's ground truth range. The radar reports lateral position accuracies as small as 0.06 meters at close ranges and up to 5.5 meters when the target is far from the radar. Multiple detections appear when the target is at ranges less than 30 meters. The target vehicle is not modeled as a single point in space, but the radar model compares the vehicle's dimensions with the radar's resolution. In this scenario, the radar views the rear side of the target vehicle. When the vehicle's rear side spans more than one of the radar's azimuth resolution cells, the radar generates detections from each resolution cell that the target occupies.

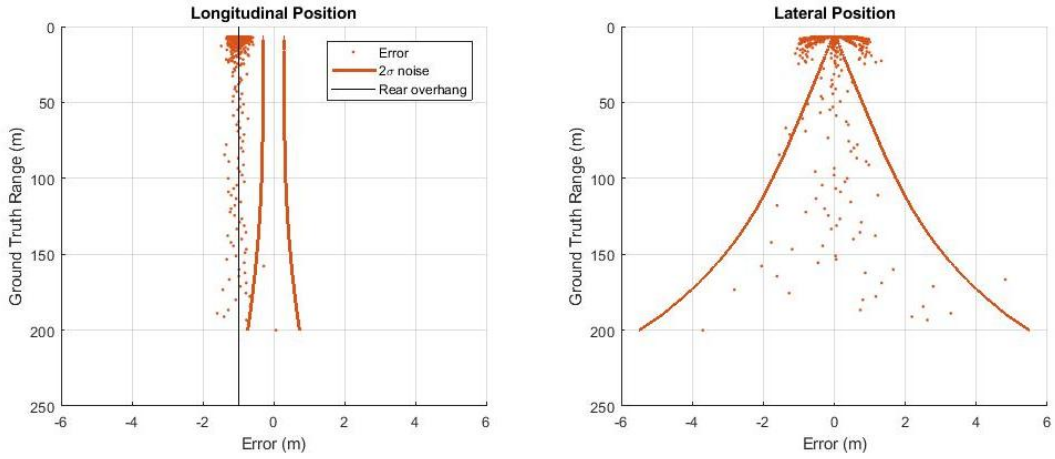

Figure 12: Error for Longitudinal & Lateral Position Measurements

If we compute the azimuth spanned by the target vehicle in the FCW Simulation when it is at 30 meters ground truth range from the ego vehicle; The azimuth spanned; azSpan = 2.9216.At a ground truth range of 30 meters, the vehicle's rear side begins to span an azimuth greater than the radar's azimuth resolution of 3^{o}. Because the azimuth spanned by the target's rear side exceeds the sensor's resolution, 3 resolved points along the vehicle's rear side are generated: one from the center of the rear side, one from the left edge of the rear side, and one from the right edge.

(iii) Target Velocity estimation-because the lead car is directly in front of the radar of the ego vehicle, it has a purely longitudinal velocity component. The passing car has a velocity profile with both longitudinal and lateral velocity components. These components change as the car passes the ego vehicle and moves into the right lane behind the lead car. To illustrate the radar's ability to observe both of these velocity components we compare the radar's measured longitudinal and lateral velocities of the target vehicles to their ground truth velocities.

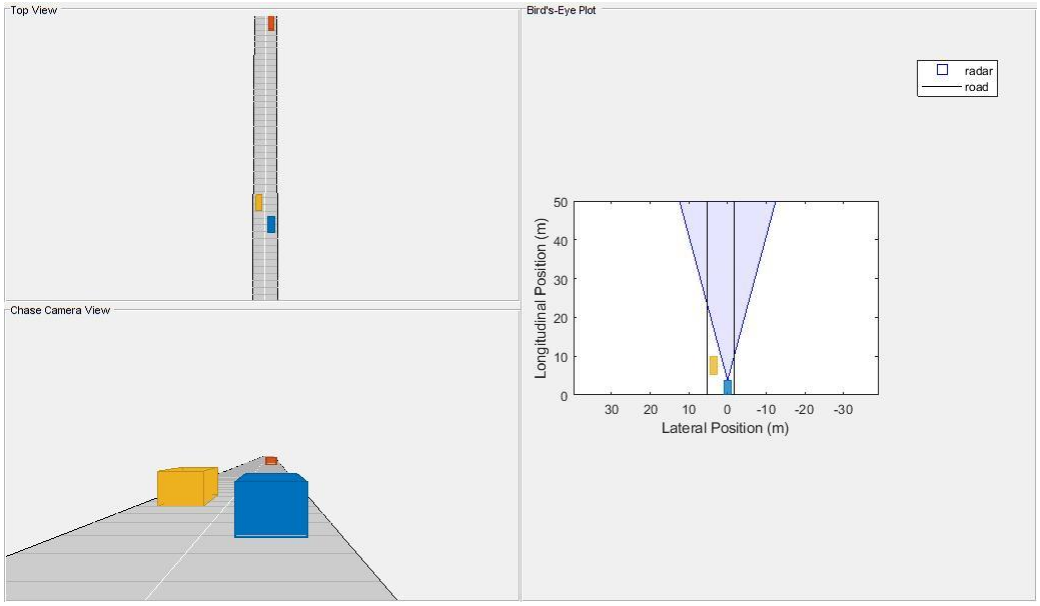

Figure 13a: Passing car just passing the ego vehicle

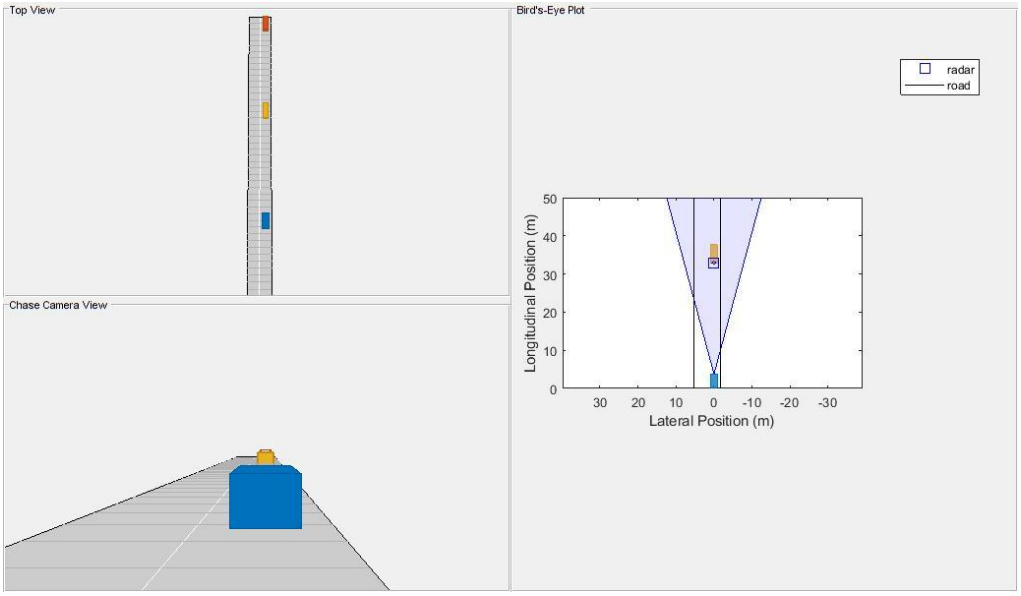

Figure 13b: Passing car just passing the ego vehicle & align to right lane

The longitudinal velocity is closely aligned to the radar's range-rate measurements, for forward-facing radar. Fig. 14 (left) shows the radar's longitudinal velocity errors for the passing vehicle scenario. Because the radar can accurately measure longitudinal velocity from the Doppler frequency shift observed in the signal energy received from both cars, the velocity errors for both vehicles (shown as points) are small. When the passing car enters the radar's field of view at 3 seconds, the passing car's 2σ measurement noise (shown using solid yellow lines) is initially large. The noise then decreases until the car merges into the right lane behind the lead car at about 6.8 seconds. As the car passes the ego vehicle, the longitudinal velocity of the passing car includes both radial and non-radial components. The ego vehicle's radar inflates its reported 2σ longitudinal velocity noise to indicate its inability to observe the passing car's non-radial velocity components as it passes the ego vehicle.

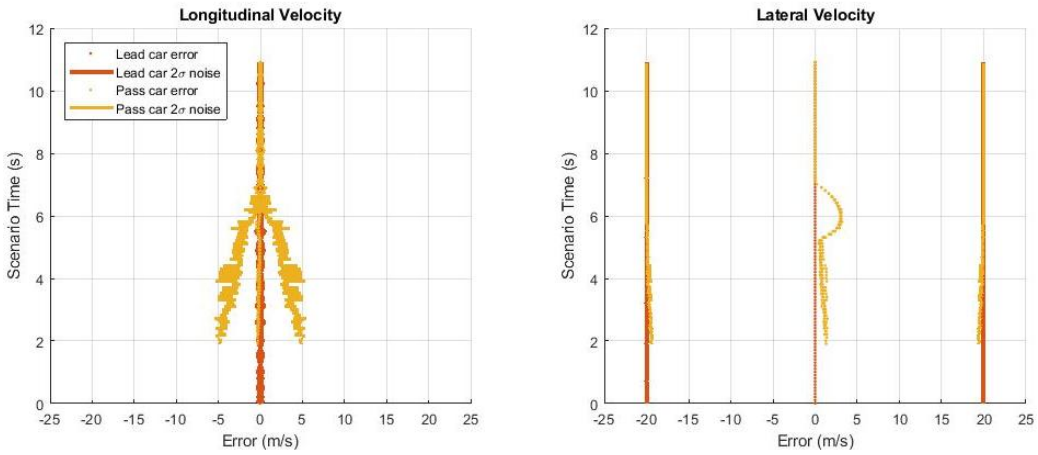

Figure 14: Error for Longitudinal & Lateral Velocity Measurements

the measured lateral velocity corresponds to a target's non-radial velocity component, for forward-facing radar. Fig. 14 (right) shows the passing car's lateral velocity measurement errors, which is displayed as yellow points. The inability of the ego vehicle radar to measure lateral velocity produces a large error during the passing car's lane change maneuver between 5 and 7 seconds. However, the radar reports a large 2σ lateral velocity noise (shown as solid lines at 20m/s) to indicate that it is unable to observe velocity along the lateral dimension.

(iv) Target Identification-plot of SNR of detections for both the target vehicle and the pedestrian;

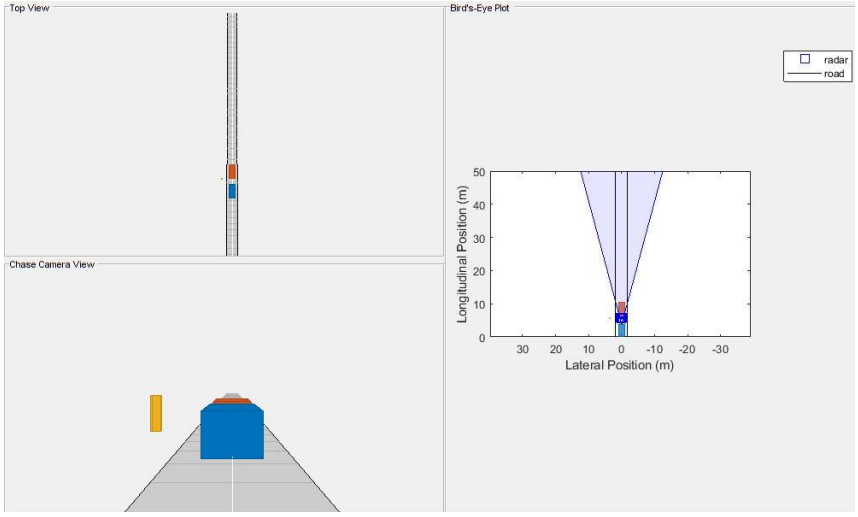

Figure 15a: Radar Pedestrian & Vehicle Detection & Stopping at 2m

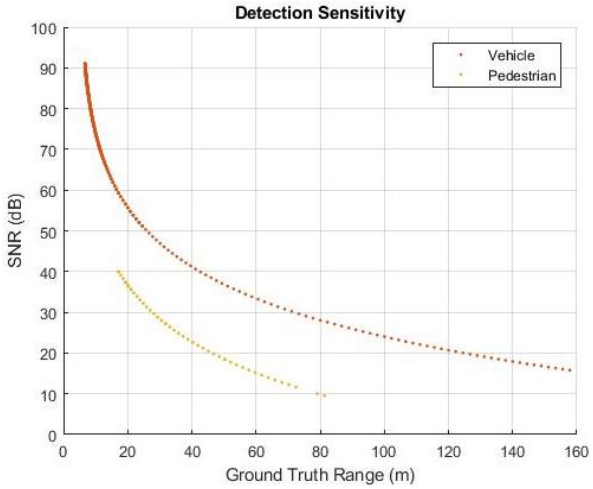

Figure 15b: SNR of Radar Pedestrian & Vehicle Detection

Analyzing the outcome of fig.15b plot shows the effect of an object's RCS on the radar's ability to "see" that object. The red dotted line shows detections corresponding to the stationary test vehicle; while the yellow is for the pedestrian. The test vehicle is detected out to the farthest range included in this simulation (160m – remember it was given detectable range of 120m), but detection of the pedestrian becomes less consistent near 75 meters. This difference between the detection range of the two objects occurs because the test vehicle has a much larger RCS (10dBsm) than the pedestrian (-8dBsm), which enables the radar to detect the vehicle at longer ranges than the pedestrian. The test vehicle is also detected at the closest range included in this test, but the radar stops generating detections on the pedestrian near 18m. In this scenario, the target vehicle is placed directly in front of the radar, but the pedestrian is offset from the radar's line of sight (LoS). Near 18 meters, the pedestrian is no longer inside of the radar's field of view and cannot be detected by the radar.

(v) *Simulation of Mid*-Range Radar Detections Performance-Carrying out the FCW simulation using the mid-range radar and the SNR for the detections from the target vehicle and pedestrian; and plot the SNR. Discussion of the simulation result from fig.16a-b below: for the mid-range radar, the detections of both the vehicle and pedestrian are limited to shorter ranges. With the long-range radar, the vehicle is detected out to the full test range, but now vehicle detection becomes unreliable at 138m. Also, the pedestrian is detected reliably only out to 37m: but there is a significant improvement in coverage over the long-range radar; the mid-range radar's extended field of view in azimuth enables detections on the pedestrian to a 7.5m ground truth range from the sensor.

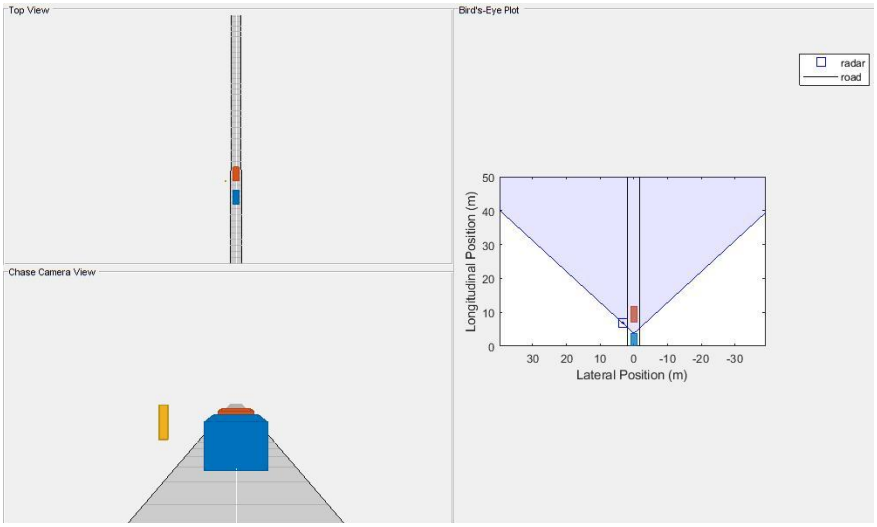

Figure 16a: Radar Pedestrian Detection less than 7.5m Ground Truth Range

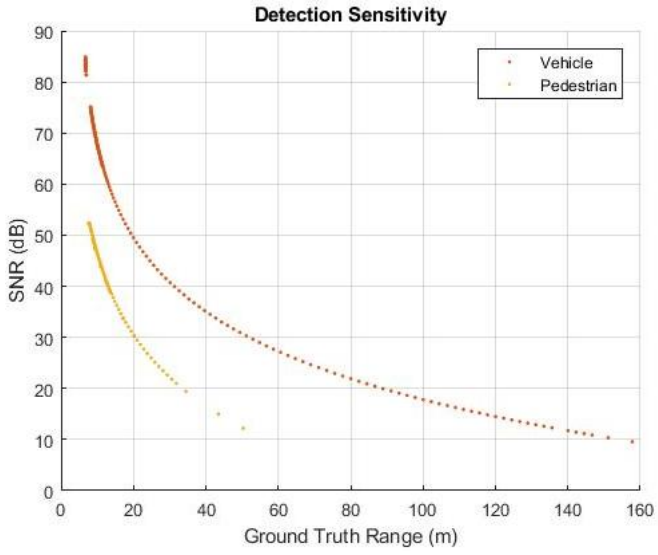

Figure 16b: SNR of Radar Pedestrian Detection less than 7.5m Ground Truth Range

(vi) *Simulating Detection of Closely Spaced Target*-the distance between the motorcycles and the ego vehicle increases with time. When the motorcycles are close to the radar, they occupy different radar resolution cells; see fig. 17a below. By the end of the scenario, after the distance between the radar and the motorcycles has increased, both motorcycles occupy the same radar resolution cells and are merged, see fig. 17b below.

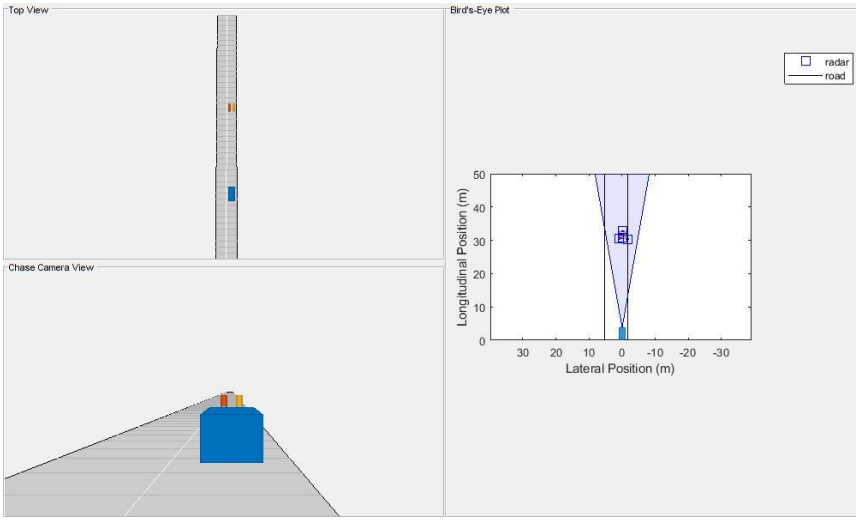

Figure 17a: Radar Detection of Closely Spaced Target (different resolution cells)

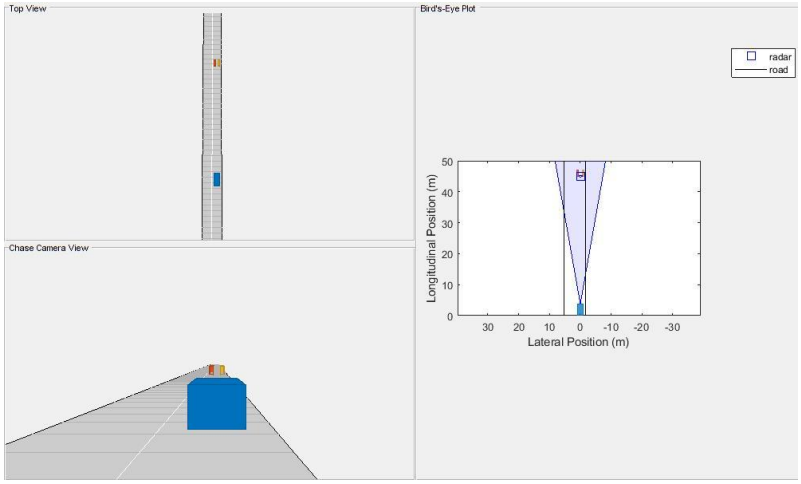

Figure 17b: Radar Detection of Closely Spaced Target (same resolution cells)

This transition that occurs during the scenario is shown by the radar's longitudinal and lateral position errors shown in fig. 17c below.

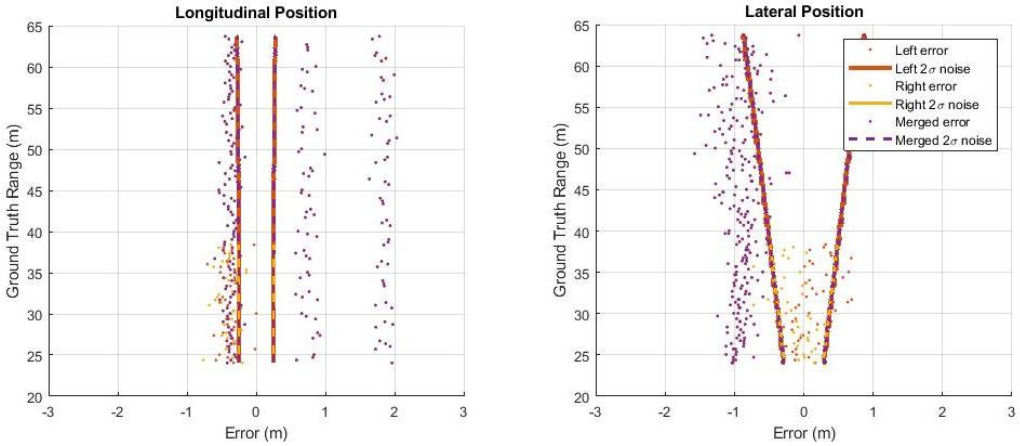

Figure 17c: Radar's longitudinal and lateral position errors

Explanation of the results: we identify the range where the radar no longer can distinguish the two motorcycles as unique objects, by analyzing the position errors reported for each motorcycle. Detections are generated from the rear and along the inner side of each motorcycle. The red errors are from the left motorcycle, the yellow errors are from the right motorcycle, and the purple points show the detections that are merged between the two motorcycles. The motorcycles are separated by a distance of 1.6m. Each motorcycle is modeled to have a width of 0.6m and a length of 2.2m. The inner sides of the motorcycles are only 1.4m apart.T he Inner Side Detections are generated from points along the inner side of each motorcycle. The detections start at the closest edge and are sampled in range according to the radar's range resolution of 2.5 meters and the motorcycle's position relative to the radar. When the motorcycle occupies multiple range resolution cells, the closest sample points in each unique range cell generate detections. The location of the range cell's boundary produces a detection that occurs either at the middle or far edge of the motorcycle's inner side. Detection from the motorcycle's closest edge is also generated. This movement through the radar's range resolution cell boundaries creates the 3 bands of longitudinal position errors seen in the preceding plot on the left. The total longitudinal extent covered by these 3 bands is 2.2 meters, which corresponds to the length of the motorcycles. Because the inner sides of the motorcycles are separated by only 1.2 meters, these sampled points all fall within a common azimuthal resolution cell and are merged by the radar. The centroid of these merged points lies in the middle of the two motorcycles. *The centroiding of the merged detections produces a -0.8m lateral bias corresponding to half of the distance between the motorcycles. In fig. 17c (right), all of the merged detections (shown in purple) have this -0.8m bias.* Rear Side Detections generated from the rear side of each motorcycle are further apart (1.6m) than the sampled points along the inner sides (1.2m).At the beginning of the simulation, the motorcycles are at a ground truth range of 24m from the ego vehicle. At this close range, detections from the rear sides lie in different azimuthal resolution cells and the radar does not merge them. These distinct rear-side detections are shown as red points (left motorcycle) and yellow points (right motorcycle) in the preceding longitudinal and lateral position error plots. For these unmerged detections, the longitudinal position errors from the rear sides are offset by the rear overhang of the motorcycles (0.37 m). The lateral position errors from the rear sides do not exhibit any bias. This result is consistent with the position errors observed in the FCW illustration.

As the simulation proceeds, the distance between the motorcycles and the radar increases, and the area spanned by the radar's resolution cells grows. When the motorcycles move beyond a ground truth range of 40m, detections generated from the rear sides of the motorcycles merge. We compute the azimuthal separation of the outside edges of the rear sides fig. 17c (left).The result of computing the azimuthal separation of the outside edges of the rear sides gives *azSep* = 3.6087.

At 39m ground truth range, the outer edges of the rear sides of the motorcycles now lie within the same 4^{o} azimuth resolution cell and are merged. Beyond this range, the two motorcycles appear to the radar as a single object and only merged detections (shown in purple) are seen in the plots of fig. 17c. This demonstration of how to model and simulate the output of automotive radars using synthetic detections, have shown how the *radarDetectionGenerator* model: (i) Provides accurate longitudinal position and velocity measurements over long ranges, but has limited lateral accuracy at long ranges; (ii) Generates multiple detections from single target at close ranges, but merges detections from multiple closely spaced targets into a single detection at long ranges; (iii) Sees vehicles and other targets with large radar cross-sections over long ranges, but has limited detections performance for nonmetallic objects such as pedestrians [31].

III. Simulation of Automotive Adaptive Cruise Control Using FMCW Technology

(i) *Simulating the FMCW Waveform*-setting up the FMCW waveform used in the radar system; this is an up-sweep linear FMCW signal, often referred to as sawtooth shape; we can examine the time-frequency plot of the generated signal, Fig. 18, below [40-43].

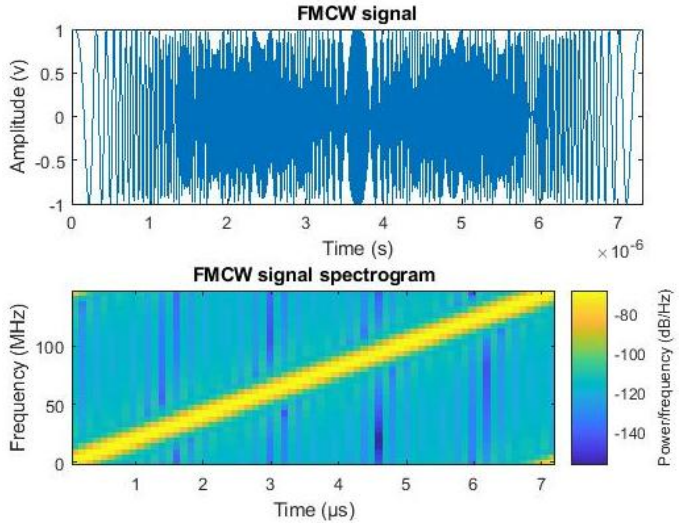

Figure 18: Time-frequency plot FMCW waveform

(ii) *Radar Signal Simulation*-FMCW radar measures the range by examining the beat frequency in the dechirped signal. To extract this frequency, a dechirp operation is performed by mixing the received signal with the transmitted signal. After the mixing, the dechirped signal contains only individual frequency components that correspond to the target range. Although it is possible to extract the Doppler information from a single sweep, the Doppler shift is often extracted among several sweeps because within one pulse, the Doppler frequency is indistinguishable from the beat frequency. FMCW radar typically performs the following operations to measure the range and Doppler:-The waveform generator generates the FMCW signal.-The transmitter and the antenna amplify the signal and radiate the signal into space.-The signal propagates to the target, gets reflected by the target, and travels back to the radar.-The receiving antenna collects the signal.-The received signal is dechirped and saved in a buffer.-Once a certain number of sweeps fill the buffer, the FT is performed in both range and Doppler to extract the beat frequency as well as the Doppler shift. One can then estimate the range and speed of the target using these results.

A total of 64 sweeps are simulated and a range Doppler response is generated at the end. A spectrum analyzer is used to show the spectrum of each received sweep as well as its dechirped counterpart during the simulation: then, run the simulation loop [40-43, 46]. From the spectrum scope, we can see that although the received signal is wideband (channel 1), sweeping through the entire bandwidth, the dechirped signal becomes narrowband (channel 2); see fig. 19 below.

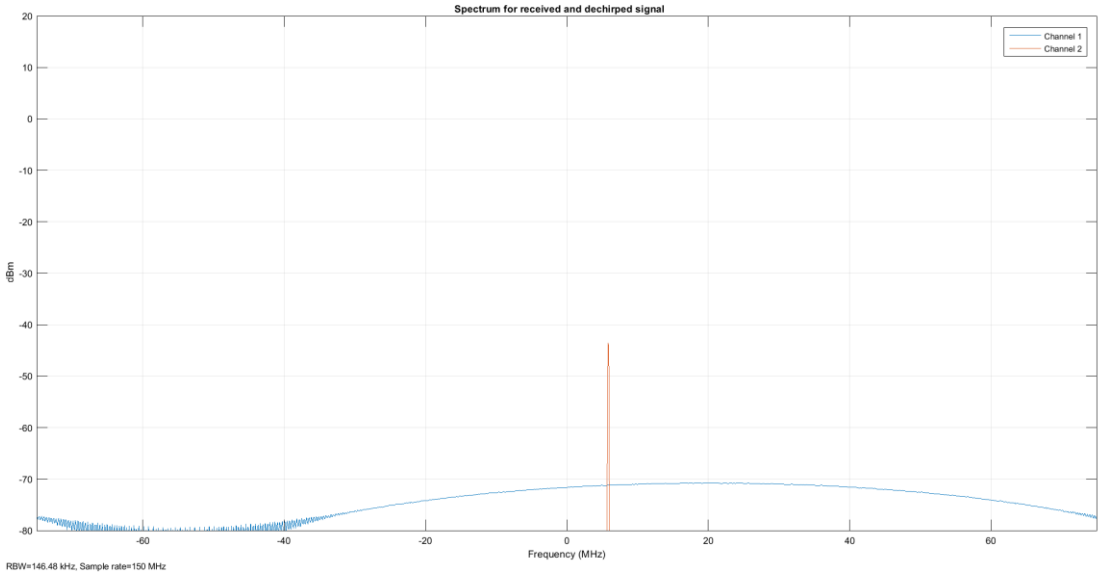

Figure 19: FMCW Radar Signal Simulation-Spectrum for received & Dechirped Signal

(iii) *Range and Doppler Estimation Simulation*-Let's take a look at the zoomed range Doppler response of all 64 sweeps before estimating the value of the range and Doppler.

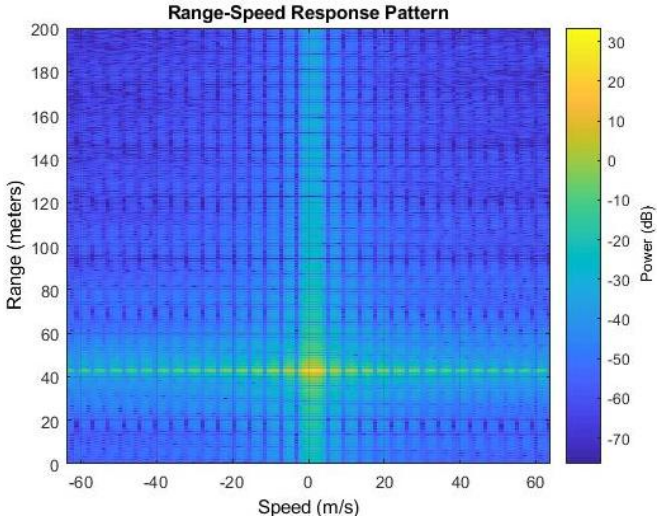

Figure 20: Zoomed Range Doppler Response

From Fig. 20 above, we see that the car in front is a bit more than 40m away and appears almost static. This is expected because the radial speed of the car relative to the radar is only 4km/h, which translates to a mere 1.11m/s. Since the maximum beat frequency is in general less than the required sweeping bandwidth, the signal can be decimated to alleviate the hardware cost; for the decimation process. To estimate the range, firstly, the beat frequency is estimated using the coherently integrated sweeps and then converted to the range: *rng_est = 42.9976*. Secondly, the Doppler shift is estimated across the sweeps at the range where the target is present: *v_est = 1.0830*. Note that both range and Doppler estimations are quite accurate [40-43, 46].

(iv) *Simulating the Range Doppler Coupling Effect*-For the situation outlined in this modeling, the range error caused by the relative speed between the target and the radar is deltaR = -0.0041. This error is so small that we can safely ignore it. To see the Range Doppler Coupling Effect, the waveform is reconfigured to use 2ms as the sweep time and calculate the range Doppler coupling: deltaR = -1.1118.A range error of 1.14 m can no longer be ignored and needs to be compensated. Naturally, one may think of doing so following the same procedure outlined in earlier sections, estimating both range and Doppler, figuring out the range Doppler coupling from the Doppler shift, and then remove the error from the estimate. Unfortunately, this process doesn't work very well with the long sweep time. The longer sweep time results in a lower sampling rate across the sweeps, thus reducing the radar's capability of unambiguously detecting high speed vehicles. For instance, using a sweep time of 2ms, the maximum unambiguous speed the radar system can detect using the traditional Doppler processing is: v_unambiguous = 0.4870. The unambiguous speed is only 0.48 m/s, which means that the relative speed, 1.11 m/s, cannot be unambiguously detected. This means that not only the target car will appear slower in Doppler processing, the range Doppler coupling also cannot be correctly compensated. To resolve such ambiguity without Doppler processing, adopt a triangle sweep pattern [40-43, 46].

(v) *Simulating the Triangular Sweep*-From the modeling in section 3.4.5, using both up sweep and down sweep beat frequencies simultaneously, the correct range estimate is obtained, when simulated: rng_est = 42.9658. Also, the Doppler shift and the velocity can also be recovered in a similar fashion: v_est = 1.1114.The range and velocity estimates match the true values, which are 43m and 1.11m/s, appropriately.

(vi) *Simulating Two-ray Propagation*-Simulating the model, with all settings remaining same, the comparison of the resulting range-Doppler map with two-ray propagation and the range-Doppler map obtained before with a LOS propagation channel suggests that the signal strength significantly dropped almost 40dB; Fig. 21 below.

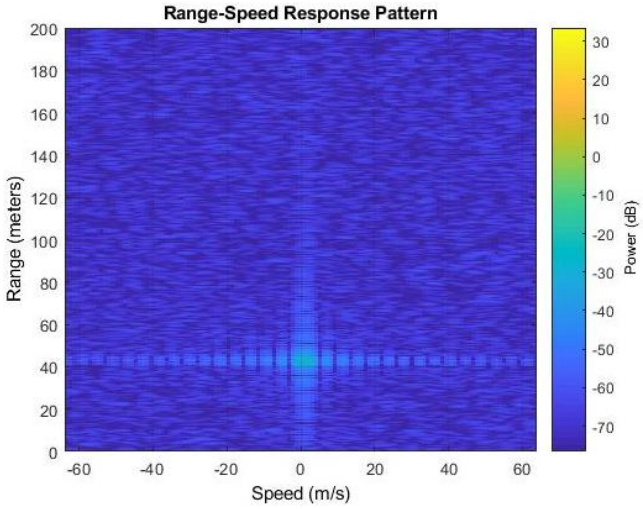

Figure 21: Multi-Path Propagation

Considering this effect during the design; a possible choice is to form a very sharp beam on the vertical direction to null out the reflections, [41], [*helperFMCWSimulate & helperFMCWTwoRaySimulate function files must be in the simulation path]*.

IV. Simulation of Automotive Radar Sensor Signal Processing with FFT

(i) *Simulating the Calculation of Radar Parameters from Long-Range Radar Requirements* Simulating the code give all expected results, proving the syntax and concepts are correct.

(ii) *Simulating the Automotive Radar Hardware*-Simulating the model, give the half power beam width as: hpbw = 16.3636. Direction of arrival is simulated to test the code for compliance; also, simulating the radar transmitter for a single transmit channel and receiver preamplifier for each receive channel, the code complies with the model.

(iii) *Simulating the Radar Signal Processing Chain*-Each set of codes; when simulated yield expected results as per the model, see the workspace window for the result of respective parameters after the simulation: the code run as modeled and without error.

(iv) *Simulating the Driving Scenario*-As modeled, simulating yield Fig. 22 below; which show the radar detections and tracks for the 3 target vehicles at 1.1 seconds of simulation time.

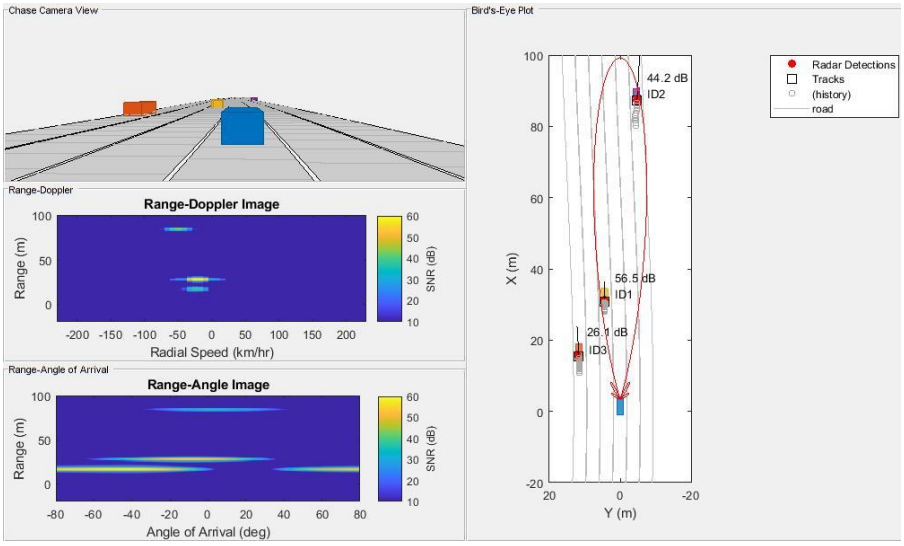

Figure 22: Simulation of ARSP with FFT – Free Space Propagation

The plot on the upper-left side shows the chase camera view of the driving scenario from the perspective of the ego vehicle (blue car). The right side of the figure shows the bird's-eye plot, which presents a "top down" perspective of the scenario. All of the vehicles, detections, and tracks are shown in the ego vehicle's coordinate reference frame. The SNR estimated for each radar measurement is printed next to each of the detections: the

vehicle location estimated by the tracker is shown in the plot using black squares with text next to them indicating each track's ID. The tracker's estimated velocity for each vehicle is shown as a black line pointing in the direction of the vehicle's velocity. The length of the line corresponds to the estimated speed, with longer lines denoting vehicles with higher speeds relative to the ego vehicle. The purple car's track (ID2) has the longest line while the yellow car's track (ID1) has the shortest line. The tracked speeds are consistent with the modeled vehicle speeds.

The two plots on the lower-left side show the radar images generated by the signal processing. The upper plot (Range-Doppler image) shows how the received radar echoes from the target vehicles are distributed in range and radial speed. Here, all three vehicles are observed. The measured radial speeds correspond to the velocities estimated by the tracker, see bird's-eye plot of Fig. 22. The lower plot (Range-Angle image) shows how the received target echoes are spatially distributed in range and angle. Again, all three targets are present, and their locations match what is shown in the bird's-eye plot. Due to its close proximity to the radar, the orange car can still be detected despite the large beam forming losses due to its position well outside of the beam's 3dB beam width. These detections have generated a track (ID3) for the orange car, [51].

(v) *Simulating the Multipath Channel*-As modeled, simulating yield Fig. 23a below; let's replace the free space channel model with a two-ray channel model to demonstrate the propagation environment, [73]. By comparing Figures 23a and 22, we observe that for the two-ray channel, no detection is present for the purple car at this simulation time (i.e. 1.1 seconds of simulation time). This detection loss is because the path length differences for this car are destructively interfering at this range, resulting in a total loss of detection.

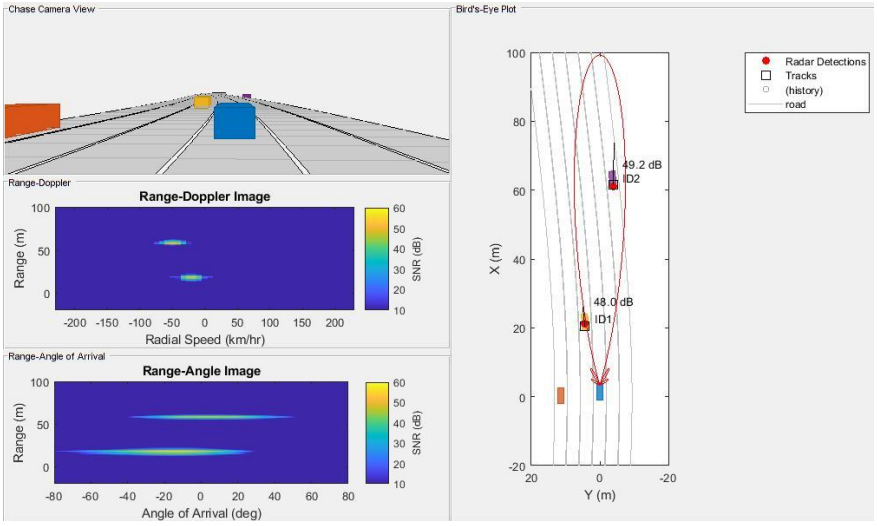

Figure 23a: Simulation of ARSP with FFT – Multipath Propagation

We plot the SNR estimates generated from the CFAR processing against the purple car's range estimates from the free space and two-ray channel simulations,[51], Fig. 23b below.

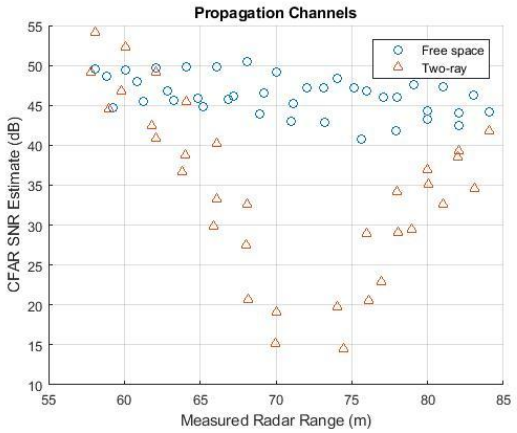

Figure 23b: SNR estimates

From Fig. 23b, we see that as the car approaches a range of 72m from the radar, a large loss in the estimated SNR from the two-ray channel is observed with respect to the free space channel. It is near this range that the multipath interference combines destructively, resulting in a loss in signal detections. However, it is observed that the tracker is able to coast the track during these times of signal loss and provide a predicted position and velocity for the purple car.

V. Problems with FFT techniques (Deduced from the reviewed Literature and theoretical background) [80]; (i) The FFT technique used in the algorithm causes the algorithm to require huge amount of intermediate data to be stored in a memory.(ii) FT technique is not suitable for non-stationary signal, except if we are only interested in what spectral components exist in the signal, but not interested where these occur. But in this application, the time localization of the spectral components is needed, a transform giving the Time-Frequency Representation of the signal is needed.(iii) The FT technique has some resolution related problems; it cannot provide the time and frequency information simultaneously, as required in this application.

VI. Problems with FFT technique (Deduced from Simulations and Analysis), [28].

(i) Poor position and velocity accuracy along the cross-range dimension-caused by: resolution and noise problems. (a) The longitudinal and lateral position errors are functions of the way the FFT process the received signals; in terms of handling the noise content and resolution issues. Radar reports lateral position accuracies as small as 0.06 meters at close ranges and up to 5.5 meters when the target is far from the radar.(b) When the passing car enters the radar's field of view, the passing car's noise is initially large. The ego vehicle's radar inflates its reported 2σ longitudinal velocity noise to indicate its inability to observe the passing car's non-radial velocity components as it passes the ego vehicle. (c) The inability of the ego vehicle radar to measure lateral velocity produces a large error during the passing car's lane change maneuver. The radar reports a large 2σ lateral velocity noise to indicate that it is unable to observe velocity along the lateral dimension.(d) Range Doppler Coupling Effect, a range error of 1.14 m can no longer be ignored and needs to be compensated – it reduces the radar's capability of unambiguously detecting high speed vehicles; even the triangle sweep pattern recommended, cannot solve this problem totally.

(ii) Shorter detection ranges for pedestrians and other nonmetallic objects-caused by: resolution problem, time-frequency issue and noise problems. The effect of an object's RCS on the radar's ability to "see" that object; cause poor detection of pedestrians and other nonmetallic objects. The mid-range radar proposed could not solve this problem too. Could be a possible cause of the incidence mentioned in introduction above.

(iii) Close range detection clusters pose a challenge to tracking algorithms-caused by: resolution problems. Multiple detections appear when the target is at ranges less than 30 meters (the radar model compares the vehicle's dimensions with the radar's resolution)

(iv) Inability to resolve closely spaced targets at long ranges-caused by: resolution problems.

After the distance between the radar and the motorcycles has increased, both motorcycles occupy the same radar resolution cells and are merged. The centroiding of the merged detections produces a -0.8m lateral bias corresponding to half of the distance between the motorcycles, all of the merged detections have this -0.8m bias.

Conclusion

This work has shown a comprehensive analysis of existing ARSP systems using FFT technique and how WT technique could be applied for the same application, to overcome some of the major set-backs of the FFT technique. From this research, I have found out that the major problems with the self-driven vehicle technology using radar sensor are in the areas of appropriate algorithm, capable chip-set and sufficient memory; to carry out the task and meet-up with the real-time processing requirement of this application. My work is focused on the area of appropriate algorithm: analyzing and listing out the problems of the existing FFT algorithm as applied in this context.

Acknowledgement

I acknowledge the following persons for their contribution to this work: Dr. A. C. Evans, Dr. Umar Sadiq, Dr. Ale Felix, Professor O. C. Ugweje, and all other contributors, who's works have aid the success of my research.

References

[1]. Ugweje, O. C. *"Advanced Communication Systems"* Class notes for EEE602, Department of Electrical and Electronics Engineering, Nile University of Nigeria, Abuja, April, 2015.

[2]. Patole, S. Torlak, M. Wang, D. and Ali, M. *"Automotive Radars. A review of signal processing techniques"* IEEE Signal Processing Magazine *Date of publication: 3rd March 2017*

[3]. Richards, M. Richards, M. A. Scheer, J. A. and Holm, W. A. *"Principles of Modern Radar: Basic Principles"*. Institution of Engineering and Technology, 2010.

[4]. Suleymanov, S. *"Design and implementation of an FMCW Radar signal processing module for automotive applications"*, M.Sc. thesis, University of Twente, 2016.

[5]. Fareez, C. W. et al *"Forward Scattering Radar (FSR) Ground Target Signal Processing Using Wavelet Technique (WT)"* in Institution of Engineering and Technology IET International Radar Conference Hangzhou, China 14-16 Oct 2015.

[6]. Sanders, F. H. *"Detection and Measurement of Radar Signals"*: A Tutorial, 7th Annual ISART, NTIA Institute for Telecommunication Sciences, 1st March 2005.

[7]. Jenn, D. (Prof.) *"Radar Fundamentals"* Department of Electrical & Computer Engineering Naval Post Graduate School, 833 Dyer Road, Room 437 Monterey, CA 93943 (831) 656-2254. jenn@nps.navy.mil, jenn@nps.eduhttp://www.nps.navy.mil/faculty/jenn

[8]. Stimson, G. *"INTRODUCTION TO AIRBORNE RADAR" BY* SCITECH PUBLICATIONS.

[9]. Semeter, J. *"Basic Radar Signal Processing"* Boston University.

[10]. Cho, J. Y. N. *"Signal Processing Algorithms for the Terminal Doppler Weather Radar: Build 2"* Project Report ATC-363. Lincoln LaboratoryMASSACHUSETTS INSTITUTE OF TECHNOLOGY Lexington, Massachusetts, February 21, 2010. Prepared for the Federal Aviation Administration,Washington, DC 20591. This document is available to the public throughthe National Technical Information Service, Springfield, VA 22161Signal.

[11]. Balghonaim, A. *"The Fourier Transform"* Class notes for EE 207 & Fourier Transform: Applications Modern Seismology – Data processing and inversion

[12]. Kim, J. *"Radar System Design Using MATLAB and Simulink"*. MATLAB® and SIMULINK R2017b Documentation. The MathWorks, Inc. *MATLAB® Primer* © COPYRIGHT 1984–2017 by The MathWorks, Inc.

[13]. Alter, J. J. & Coleman, J. O. *Radar Digital Signal Processing"*. Naval Research Laboratory.

[14]. Jonas Gomes & Luiz Velho *"From Fourier Analysis to Wavelets"*. Instituto de Matematica Pura e Aplicada, IMPA Rio de Janeiro, Brazil.

[15]. Polikar, R.*"The Wavelet Tutorial"* Second Edition, Part I— Fundamental Concepts & an Overview of the Wavelet Theory. 1996.

[16]. Polikar, R. *"The Wavelet Tutorial"* Second Edition, Part II— Fundamentals: the Fourier Transform and the Short Term Fourier Transform. 1996.

[17]. Polikar, R.*"The Wavelet Tutorial"* Second Edition, Part III— Multi-Resolution Analysis & the Continuous Wavelet Transform. 1996.

[18]. Polikar, R.*"The Wavelet Tutorial"* Second Edition, Part IV— Multi-Resolution Analysis: the Discrete Wavelet Transform. 1996.

[19]. Daubechies, I. Meyer, Y. & Mallat, S.*"Basics of Wavelets"* Ten Lectures on Wavelets; Orthonormal Bases of Compactly Supported Wavelets.

[20]. Misiti, M. et al *"Wavelet Toolbox"* For Use with MATLAB®.

[21]. Gilbert, S. & Nguyen, Truong. *"Wavelets and Filter Banks"*. Wellesley, MA: Wellesley-Cambridge Press, 1996.

[22]. Vaidyanathan, P. P. *"Multirate Systems and Filter Banks*". Englewood Cliffs, New Jersey: Prentice Hall PTR, 1993.

[23]. Lee, T. L. & Akio Yamamoto *"Wavelet Analysis: Theory & Application"*. Hewlett-Packard Journal, December 1994.

[24]. Parrish, K.*"An Overview of FMCW Systems in MATLAB"* Research Gate Article. May 2010 https://www.researchgate.net/publication/260286270
[25]. Barrick, D. N. Oceanic, and A. A. W. P. Lab, "*FM/CW Radar Signals and Digital Processing"*. Environmental Research Laboratories, 1973.
[26] Stove, A. *"Linear FMCW radar techniques,"* in IEEE Proceedings on Radar and Signal Processing, vol. 139, no. 5, 1992, pp. 343–350.
[27]. https://www.youtube.com/watch?v=dY8xeuZWu5U Mar 21, 2018 - Uploaded by TARNews923.
[28]. Nathaniel U. N., Evans C. A., Abubakar U. S. "*Modeling, Simulation & Analysis of the Applicability of Wavelet Transform Technique for Automotive Radar Signal Processing".* Paper Published in International Journal of Scientific and Engineering Research (IJSER) Volume 10, Issue4, April 2019 Edition (ISSN 2229-5518), pages 541-554.
[29]. Karnfelt, C. et al. "*77 GHz ACC Radar Simulation Platform*", IEEE International Conferences on Intelligent Transport Systems Telecommunications (ITST), 2009.
[30]. The MATLAB® Documentation: "*Sensor Fusion Using Synthetic Radar and Vision Data*". MATLAB® and SIMULINK R2017b Documentation. The MathWorks, Inc. *MATLAB® Primer* © COPYRIGHT 1984–2017 by The MathWorks, Inc.
[31]. The MATLAB® Documentation: "*Model Radar Sensor Detections*". MATLAB® and SIMULINK R2017b Documentation. The MathWorks, Inc. *MATLAB® Primer* © COPYRIGHT 1984–2017 by The MathWorks, Inc.
[32]. The MATLAB® Documentation: "*Radar Equation Calculator*". MATLAB® and SIMULINK R2017b Documentation. The MathWorks, Inc. *MATLAB® Primer* © COPYRIGHT 1984–2017 by The MathWorks, Inc.
[33]. The MATLAB® Documentation: "*Driving Scenario Generation and Sensor Models*". MATLAB® and SIMULINK R2017b Documentation. The MathWorks, Inc. *MATLAB® Primer* © COPYRIGHT 1984–2017 by The MathWorks, Inc.
[34]. The MATLAB® Documentation: "*Detection, Range and Doppler Estimation*". MATLAB® and SIMULINK R2017b Documentation. The MathWorks, Inc. *MATLAB® Primer* © COPYRIGHT 1984–2017 by The MathWorks, Inc.
[35]. The MATLAB® Documentation: *"Visualize Sensor Coverage, Detections, and Tracks".* MATLAB® and SIMULINK R2017b Documentation. The MathWorks, Inc. *MATLAB® Primer* © COPYRIGHT 1984–2018 by The MathWorks, Inc.
[36]. The MATLAB® Documentation: *"Doppler Estimation".* MATLAB® and SIMULINK R2017b Documentation. The MathWorks, Inc. *MATLAB® Primer* © COPYRIGHT 1984–2018 by The MathWorks, Inc.
[37]. The MATLAB® Documentation: *"Driving Scenario Tutorial".* MATLAB® and SIMULINK R2017b Documentation. The MathWorks, Inc. *MATLAB® Primer* © COPYRIGHT 1984–2018 by The MathWorks, Inc.
[38]. The MATLAB® Documentation: *"Create Actor and Vehicle Paths".* MATLAB® and SIMULINK R2017b Documentation. The MathWorks, Inc. *MATLAB® Primer* © COPYRIGHT 1984–2018 by The MathWorks, Inc.
[39]. The MATLAB® Documentation: *"Zoom FFT".* MATLAB® and SIMULINK R2017b Documentation. The MathWorks, Inc. *MATLAB® Primer* © COPYRIGHT 1984–2018 by The MathWorks, Inc.
[40]. [40] Richards, Mark. "*Fundamentals of Radar Signal Processing"*. New York: McGraw Hill, 2005.
[41]. The MATLAB® Documentation: *Automotive Adaptive Cruise Control Using FMCW Technology*. MATLAB® and SIMULINK R2017b Documentation. The MathWorks, Inc. *MATLAB® Primer* © COPYRIGHT 1984–2018 by The MathWorks, Inc.
[42]. Karnfelt, C. et al. "*77 GHz ACC Radar Simulation Platform*", IEEE International Conferences on Intelligent Transport Systems Telecommunications (ITST), 2009.

[43]. The MATLAB® Documentation: *"Automotive Adaptive Cruise Control Using FMCW and MFSK Technology".* MATLAB® and SIMULINK R2017b Documentation. The MathWorks, Inc. *MATLAB® Primer* © COPYRIGHT 1984–2018 by The MathWorks, Inc.

[44]. The MATLAB® Documentation: *"FMCW Patch Antenna Array".* MATLAB® and SIMULINK R2017b Documentation. The MathWorks, Inc. *MATLAB® Primer* © COPYRIGHT 1984–2018 by The MathWorks, Inc.

[45]. The MATLAB® Documentation: *"Patch Antenna Array for FMCW Radar".* MATLAB® and SIMULINK R2017b Documentation. The MathWorks, Inc. *MATLAB® Primer* © COPYRIGHT 1984–2018 by The MathWorks, Inc.

[46]. Rohling, H. and Meinecke, M.. "*Waveform Design Principle for Automotive Radar Systems*", Proceedings of CIE International Conference on Radar, 2001.

[47]. The MATLAB® Documentation: "*Transmitter*". MATLAB® and SIMULINK R2017b Documentation. The MathWorks, Inc. *MATLAB® Primer* © COPYRIGHT 1984–2017 by The MathWorks, Inc.

[48]. The MATLAB® Documentation: "*Receiver Preamp*". MATLAB® and SIMULINK R2017b Documentation. The MathWorks, Inc. *MATLAB® Primer* © COPYRIGHT 1984–2017 by The MathWorks, Inc.

[49]. The MATLAB® Documentation: *"Range Estimation Using Stretch Processing".* MATLAB® and SIMULINK R2017b Documentation. The MathWorks, Inc. *MATLAB® Primer* © COPYRIGHT 1984–2018 by The MathWorks, Inc.

[50]. The MATLAB® Documentation: *"Modeling the Propagation of RF Signals".* MATLAB® and SIMULINK R2017b Documentation. The MathWorks, Inc. *MATLAB® Primer* © COPYRIGHT 1984–2018 by The MathWorks, Inc.

[51]. The MATLAB® Documentation: "*Radar Signal Simulation and Processing for Automated Driving*". MATLAB® and SIMULINK R2017b Documentation. The MathWorks, Inc. *MATLAB® Primer* © COPYRIGHT 1984–2017 by The MathWorks, Inc.

[52]. The MATLAB® Documentation: *"Signal Detection Using Multiple Samples".* MATLAB® and SIMULINK R2017b Documentation. The MathWorks, Inc. *MATLAB® Primer* © COPYRIGHT 1984–2018 by The MathWorks, Inc.

[53]. The MATLAB® Documentation: *"Radar Data Cube".* MATLAB® and SIMULINK R2017b Documentation. The MathWorks, Inc. *MATLAB® Primer* © COPYRIGHT 1984–2018 by The MathWorks, Inc.

[54]. The MATLAB® Documentation: *"Constant False Alarm Rate (CFAR) Detection".* MATLAB® and SIMULINK R2017b Documentation. The MathWorks, Inc. *MATLAB® Primer* © COPYRIGHT 1984–2018 by The MathWorks, Inc.

[55]. The MATLAB® Documentation: *"Signal Detection in White Gaussian Noise".* MATLAB® and SIMULINK R2017b Documentation. The MathWorks, Inc. *MATLAB® Primer* © COPYRIGHT 1984–2018 by The MathWorks, Inc.